Molecular orientation and the infrared dichroism of a chiral smectic liquid crystal in a homogeneously aligned cell at different temperature and bias fields

A. A. Sigarev,[1,*] J. K. Vij,[1,†] R. A. Lewis,[2] M. Hird,[2] and J. W. Goodby[2]
[1]*Department of Electronic and Electrical Engineering, Trinity College, University of Dublin, Dublin 2, Ireland*
[2]*School of Chemistry, University of Hull, Hull, United Kingdom*

(Received 10 February 2003; published 26 September 2003; publisher error corrected 6 November 2003)

The molecular orientation and the dichroic behavior of the vibrational bands of a homogeneously aligned helical cell containing chiral smectic liquid crystal (R)-(-)-1-methylheptyl 4-(4′-dodecyloxybiphenyl-4-ylcarbonyloxy)-3-fluorobenzoate are studied at various temperatures as a function of the bias field. These temperatures correspond to the various phase states of the sample at zero field. For those bands that exhibit significant dichroism, the field dependencies of the dichroic parameters (the dichroic ratio and the polarization angle of maximum absorbance) are found to be dependent on temperature, phase state, and helical unwinding. For the SmA^* and SmC^*_α phases, the phenyl band dichroic ratio and the corresponding orientational order parameter are found to be almost independent of the bias field. The temperature dependence of the orientational order for zero field is discussed by taking into account the structures of the phases and the molecular tilt angles. The field dependencies of the phenyl band dichroic parameters for the SmC^*_A and SmC^*_γ phases yield results about the distribution of directors in the layers of their unit cells and the state of helical unwinding. The azimuthal orientational distribution function of the carbonyl transition moments with respect to the long molecular axis has been determined. It is found that the degrees of the polar and quadrupolar biasing increase with decrease in temperature and the azimuthal biasing angle for the chiral carbonyl group increases significantly with a reduction in temperature.

DOI: 10.1103/PhysRevE.68.031707 PACS number(s): 61.30.Gd, 42.70.Df, 77.80.−e, 78.30.−j

I. INTRODUCTION

The determination of the molecular arrangement in the various phases of ferroelectric and antiferroelectric liquid crystals (FLCs and AFLCs) in aligned cells is an important problem not only for the correct identification of these phases but also for advancing the understanding of the physical processes that occur in samples when subjected to external conditions. These include temperature, electric field, boundary effects, surfaces, etc. Recent studies on free standing films by x-ray scattering [1] and ellipsometry [2,3] confirmed the existence of two-, three-, and four-layer periodicities in the chiral smectic phases C_A (SmC^*_A), SmC^*_γ (SmC^*_{FI1}), and AF (SmC^*_{FI2}), respectively. These studies have shown that the structures of phases with well defined layer periodicities follow the deformed clock model. Work on homeotropic aligned samples using ellipsometry [2] and optical rotatory power [4,5] has shown that the distortion from the one-dimensional Ising model is very small and in the case of SmC^*_{FI1} and SmC^*_{FI2} the distortion angle is less than 10°. Fukuda and co-workers [6,7] gave a possible general sequence of ferro-, ferri-, and antiferroelectric liquid crystalline phases for chiral smectic materials on cooling from the paraelectric smectic A phase (SmA^*) as follows: SmA^*–SmC^*_α–SmC^*–spr1–AF (SmC^*_{FI2})–spr2–SmC^*_γ (SmC^*_{FI1})–spr3–SmC^*_A. The abbreviations spr1, spr2, and spr3 designate the subphase regions or subphases in the temperature intervals between the respective neighboring phases in this sequence. In our earlier works, we called a ferroelectric phase in the subphase region spr1 [between the ferroelectric smectic C phase (SmC^*) and the antiferroelectric phase AF] the FiLC subphase [8] and also the SmC^*_{FI3} phase [9]. It may be stated that the phase sequence exhibited by a particular compound depends on the compound itself, its optical purity, and the boundary conditions of the cell configuration including its thickness. A compound in a given cell configuration may not therefore exhibit all phases and subphases as mentioned above [6,7]. A field across the cell can also induce phases by disturbing the energy equilibrium between the ferro- and the antiferroelectric ordering, and can introduce structural transitions in a sample by unwinding the helical structure and by affecting the chevron, bookshelf, and twisted structures.

The electric-field dependencies of the various physical properties (for example, the conoscopic image, apparent tilt angle, effective macroscopic polarization, dielectric, pyroelectric, and electro-optic measurements, etc.) are used for characterizing the phases at zero field, for observing the field-induced phase transitions, and for investigating the fluctuations and spatial distribution of the molecular directors in a cell [10,11]. Fourier-transform infrared (FTIR) spectroscopy is a powerful technique complementary to some of the techniques mentioned here. Polarized FTIR spectroscopy is used to analyze anisotropic organic materials, including polymers [12] and liquid crystals [13–18]. The existence of biasing in the azimuthal distribution of carbonyl groups about the long molecular axis was confirmed for unwound SmC^* structures from the IR dichroic behavior of the phenyl

*Permanent address: Research Institute of Physical Problems, Moscow, 124460, Russia.
†Author to whom correspondence should be addressed. Electronic address: jvij@tcd.ie

and carbonyl bands [13–18]. Polarized time-resolved FTIR spectroscopy has been used for studying the dynamics of the molecular reorientation in FLCs and AFLCs under alternating electric fields [13,18]. Studies of homeotropically aligned cells may give information about the validity of the distorted Ising model or the distorted clock model for the short-pitch structures of various smectic phases as well as about the biased orientational distributions of directors for rather low electric fields.

The rotational bias in the azimuthal distribution of the carbonyl groups about the molecular long axis was found from the investigations of the infrared dichroic data [17] for the SmC^*_{FI3} phase (designated as FiLC in Ref. [8]) existing in the temperature range between SmC^* and AF (SmC^*_{FI2}) phases in a chiral smectic liquid crystal (LC) (*R*)-(-)-1-methylheptyl 4-(4′-dodecyloxybiphenyl-4-ylcarbonyloxy)-3-fluorobenzoate. The degree of rotational biasing was found [17] to be rather low compared to those in other FLCs and AFLCs studied so far [15,16]. The orientational order parameter for the ensemble of molecules can be determined from the IR dichroism of the phenyl band at wave number $\sim 1600\ \mathrm{cm}^{-1}$, the transition moment of which is almost parallel to the molecular director. The rotational orientational distribution of the molecules is determined by solving a set of equations for the dichroic data of the phenyl and other bands. For the latter the transition moments should make large polar angles with the molecular long axis [13–17]. Although in a homogeneously aligned helical cell at zero field the averaged orientation of the molecular directors is observed to be almost similar for different tilted phases due to the helical structure, nevertheless the response of the LC sample to the electric field is dependent on the phase state at zero field. For infrared absorption spectroscopy, the response of a planar LC cell is observed in terms of the changes in the parameters of the anisotropic absorbance profile. These are the dichroic ratios and the orientations of the symmetry axes of the absorbance profile.

In this paper, polarized FTIR spectroscopy is used for structural studies of a chiral smectic liquid crystal in a thin homogeneously aligned helical cell. The absorption anisotropy of several characteristic vibrational bands is investigated for various temperatures and electric fields. The observed voltage dependencies of the dichroic parameters for various phase states at zero field (i.e., the sample at different temperatures) are interpreted in terms of the molecular orientational distribution of the directors in the various layers. The experimental dichroic data for the field-induced SmC^* phase for the unwound structure are used in determining the biasing parameters of the azimuthal distribution function of the carbonyl transition moments as a function of temperature. A systematic determination of the dichroic and biasing parameters, as a function of both temperature and bias field for a compound that exhibits several phases, is carried out.

II. EXPERIMENT

A chiral smectic liquid crystal (*R*)-(-)-1-methylheptyl 4-(4′-dodecyloxybiphenyl-4-ylcarbonyloxy)-3-fluorobenzoate (acronym 12OF1M7) with the following structural formula and phase sequence under slow cooling is investigated.

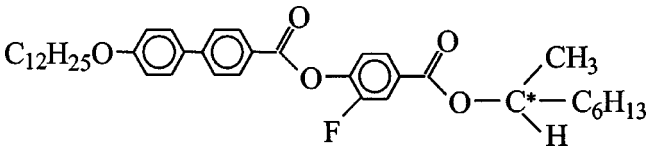

$$\mathrm{Iso} \underset{106\,^\circ\mathrm{C}}{\rightarrow} \mathrm{Sm}A^* \underset{94.5\,^\circ\mathrm{C}}{\rightarrow} \mathrm{Sm}C^*_{\alpha} \underset{93\,^\circ\mathrm{C}}{\rightarrow} \mathrm{Sm}C^* \underset{92\,^\circ\mathrm{C}}{\rightarrow} \mathrm{FiLC} \underset{85.5\,^\circ\mathrm{C}}{\rightarrow} \mathrm{AF}$$
$$\underset{80.5\,^\circ\mathrm{C}}{\rightarrow} \mathrm{Sm}C^*_{\gamma} \underset{77\,^\circ\mathrm{C}}{\rightarrow} \mathrm{Sm}C^*_{A} \underset{\sim 55\,^\circ\mathrm{C}}{\rightarrow} \mathrm{cryst.}$$

This compound was resynthesized in Hull (U.K.) with a higher optical purity in comparison with the sample used earlier in [8,17]. This is confirmed by the existence of a ferroelectric phase SmC^*_{α} in the temperature range between SmA^* and SmC^* and a ferrielectric phase SmC^*_{γ} over a relatively extended temperature interval. The given phase sequence was determined from measurements of the pyroelectric response in a cell of 15 μm thickness on cooling at a rate of 0.1 °C per min [19]. However, dielectric studies show that the AF phase is suppressed by the surfaces in a thin enough cell (thickness $\leqslant 8$ μm) [8], and the temperature range 85.5–80.5 °C corresponds to the adjacent phases FiLC (~92–85 °C) and SmC^*_{γ} (85–~80 °C). This result is important for the FTIR transmission technique at normal incidence since the absorbance profiles of strong IR bands for well aligned LC cells can be measured with sufficient accuracy only if the cell thickness does not exceed 7–8 μm.

A homogeneously aligned sample of the compound was prepared by a method similar to that described in [17]. A cell of 6 μm sample thickness was made using CaF_2 windows coated with a thin conducting layer of indium tin oxide (ITO) and an aligning layer of nylon 6,6. The latter was spin coated over ITO electrodes using a solution in methanol and dried at 100 °C. Both substrates were rubbed in one direction. A bookshelf structure was obtained for the sample between CaF_2 substrates. Nevertheless, a striped-bookshelf layer structure was obtained for the same FLC compound when a cell with ZnSe substrates [17] was used. The homogeneity in the sample's structure was examined using polarized optical microscopy. After cooling the sample to the SmC^* phase at zero field, the chevron structure was transformed to a bookshelf structure through application of a sufficiently large electric field. The cell of 6 μm thickness exhibited a helical structure for the tilted phases at zero field.

The absorption spectra in the wave number range $1000-4000\ \mathrm{cm}^{-1}$ were measured at several temperatures (see Table I) using the experimental setup as before [17]. Temperatures were chosen to lie within the temperature ranges that correspond to SmA^*, SmC^*_{α}, SmC^*, FiLC, SmC^*_{γ}, and SmC^*_{A}. Figure 1 shows the schematic of a LC cell in the laboratory coordinate system. An IR polarized beam is incident normally on the windows of the cell. The orientations of the molecules and the transition moments are described by the angles Θ, φ, β, and γ. The smectic layer normal in a cell was found from the absorbance anisotropy of the phenyl band for the SmA^* phase at zero field. A signal-to-noise ratio greater than 2000 was achieved by av-

TABLE I. Dichroic parameters $\Omega_{max}(0)$, $\Omega_{max}(U_S)$, and $\Delta\Omega_{max}(U_S)$ for the bands at 1604, 1722, and 1747 cm^{-1} for a 6 μm cell of 12OF1M7 at several temperatures.

T (°C)	Phase for zero field	Band (cm^{-1})	$\Omega_{max}(0)$ (deg)	$\Omega_{max}(U_S)$ (deg)	$\Delta\Omega_{max}(U_S)$ (deg)	U_S (V)
		1604	0.5	14.8	14.3	
94	SmC^*_α	1722	90.7	101.4	10.7	~50
		1747	0	25.9	25.9	
		1604	−0.7	16.7	17.3	
92.5	SmC^*	1722	88.8	102.9	14.1	10
		1747	−10.5	28.8	39.3	
		1604	−0.3	24.7	25.0	
85.5	FiLC	1722	90.7	109.0	18.3	11
		1747	−15.4	41.5	56.9	
		1604	0.2	26.5	26.3	
79	SmC^*_γ	1722	90.2	109.9	19.7	20
		1747	59.6	44.4	−15.2	
		1604	−0.1	26.9	27.0	
68	SmC^*_A	1722	89.8	108.0	18.2	26
		1747	14.6	47.1	32.5	

eraging 16 scans recorded for a spectral resolution of 2 cm^{-1}. For a fixed temperature, the spectral measurements were carried out by increasing dc bias voltage across the cell from zero to a value sufficient to create the induced SmC^* phase and also unwind the helix. For a fixed voltage, a set of polarized spectra was recorded for the polarization angles Ω

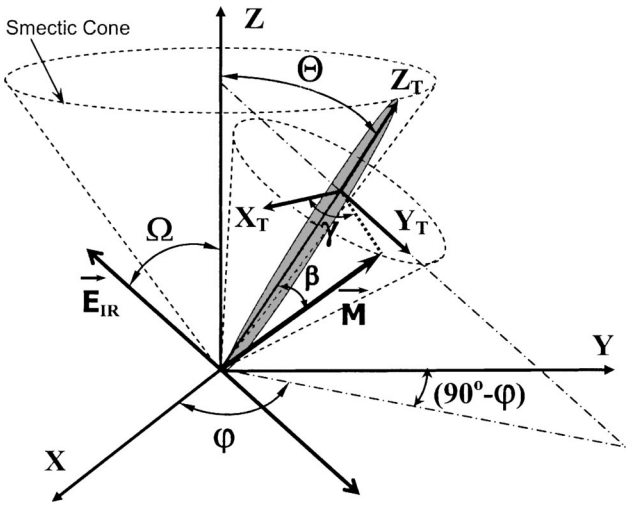

FIG. 1. The scheme of the orientations of a cell, molecules, and transition moments in the laboratory frame (X,Y,Z): the X axis is normal to the cell substrates and lies along the IR radiation propagation direction, the Z axis is along the smectic layer normal, and Ω is the angle of the Z axis with the electric vector $\mathbf{E}_{IR}$ of polarized IR radiation. (X_T,Y_T,Z_T) is the liquid crystal molecular frame: the Z_T axis is parallel to the molecular long axis and makes the polar angle Θ with the Z axis and the azimuthal angle φ with the X axis and the (Y_T,Z_T) plane is parallel to the molecular tilt plane. The transition moment $\mathbf{M}$ of a certain vibration is characterized by the polar angle β with respect to the molecular long axis and the azimuthal angle γ measured from the X_T axis.

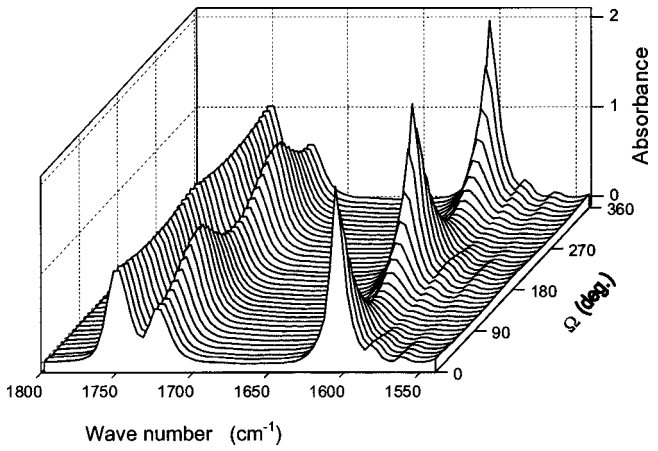

FIG. 2. A set of polarized IR spectra for a 6 μm cell of 12OF1M7 in SmA^* at 98 °C and zero field for a number of polarizer rotation angles Ω (in the range 0°–360°).

that were varied in steps of 10°. As an example, Fig. 2 shows a set of polarized IR spectra of the compound in SmA^* for various polarization angles Ω. The dichroic properties of the sample for four absorption bands listed in Table II are analyzed. These bands belong to the stretching vibrations of the phenyl ring, the bands of the two different carbonyl groups, and the asymmetric vibrations of the methylene groups.

Prior to the spectral data recording, various phases of 12OF1M7 for zero field at the temperatures used (see Table I) were confirmed through the observation of the voltage dependencies of the normalized macroscopic polarization P^*/P_S. The polarization (Fig. 3) was measured using the reversed current method [20]. At 94 °C in the SmC^*_α phase, P^*/P_S increases monotonically with field and then saturates at a field of ~8 V/μm. This field is considerably higher than the saturating field for tilted phases at lower temperatures. We note here that the voltage dependencies of P^*/P_S and the IR dichroic parameters of a 6 μm cell in a temperature range 80.5 to 85 °C (which otherwise corresponds to the AF phase in a thick cell at zero field) are observed for the SmC^*_γ phase. In the range of 85–~92 °C these dependencies correspond to the FiLC phase. This agrees with the results of the dielectric studies [8], where the AF phase was suppressed for cell thicknesses ≤8 μm.

III. THEORETICAL CONSIDERATIONS

A. Molecular structure

The structural properties of the compound 12 OF1M7 have already been given in [17]. The central core and the hydrocarbon tails form a bent zigzaglike molecular structure, typical of a number of chiral FLC compounds. Molecular modeling shows that the *para* axes of the phenyl and biphenyl segments make an angle of ~10° with each other, and these axes are also directed at an angle of 12° to the molecular long axis. Hence $\beta_{1604}=12°$ and a single value of the transition moment of the vibrations of both the phenyl and the biphenyl segments is used here. For the phenyl ring C-C symmetric stretching vibrations at 1604 cm^{-1}, the transition moment is parallel to the *para* axis of the phenyl ring [21].

TABLE II. Assignments of several absorption bands in IR spectra of 12OF1M7.

Band (cm^{-1})	Group	Type of vibrations
1604	Phenyl ring	In-plane C—C stretching
1722	C═O (near the chiral center)	Stretching
1747	C═O (in the core part)	Stretching
2927	CH_2	Asymmetric stretching

For the carbonyl groups situated near the chiral center (the ''chiral'' carbonyl) and lying in the core part of a molecule (the ''core'' carbonyl), the C═O bonds make angles of ~76° and ~68° with the molecular long axis, respectively. However, the transition moments of the C═O stretching vibrations are not parallel to their respective carbonyl bonds and these can make angles varying from 10° to 20° with their bonds [12]. β_{1722} and β_{1747} for the C═O transition moments determined from the analysis of the dichroic data for the carbonyl and the phenyl bands are given in Sec. IV B.

The axes of the two hydrocarbon tails are not parallel to each other and these make polar angles of ~25°–30° with the molecular long axis. The transition moments of the methylene asymmetric stretching vibrations are almost normal to the plane containing a zigzaglike chain of C atoms of a hydrocarbon tail [12] and make polar angles of approximately 60° and 70° for the C_6H_{13} and the $C_{12}H_{25}$ chains, respectively.

B. Dichroic properties

1. Absorbance parameters

For an ideal bookshelf geometry, the axis of a helical structure in a cell is parallel to the smectic layer normal (Z axis in Fig. 1). The absorbances A_Y, A_Z, and A_{YZ} for a particular band are defined by the relations

$$A_Y = k\langle M_Y^2\rangle/|\mathbf{M}|^2, \quad A_Z = k\langle M_Z^2\rangle/|\mathbf{M}|^2,$$
$$A_{YZ} = k\langle M_Y M_Z\rangle/|\mathbf{M}|^2, \tag{1}$$

the coefficient k characterizes the band intensity, and $|\mathbf{M}|$ is the modulus of the vector $\mathbf{M}$. Using general expressions for the components M_Y and M_Z of a transition moment $\mathbf{M}$ in the laboratory coordinate system (X,Y,Z) in terms of the angles Θ, φ, β, and γ [17], the absorbances (1) can be expressed as follows:

$$\begin{aligned} A_Y = k\{&\sin^2\beta\langle\cos^2\gamma\rangle + \langle\sin^2\varphi\rangle(\cos^2\beta\langle\sin^2\Theta\rangle \\ &+ \sin^2\beta\langle\cos^2\Theta\rangle\langle\sin^2\gamma\rangle - \sin^2\beta\langle\cos^2\gamma\rangle \\ &+ 2\sin\beta\cos\beta\langle\sin\Theta\cos\Theta\rangle\langle\sin\gamma\rangle) \\ &- 2\sin\beta\langle\sin\varphi\cos\varphi\rangle(\cos\beta\langle\sin\Theta\rangle\langle\cos\gamma\rangle \\ &+ \sin\beta\langle\cos\Theta\rangle\langle\sin\gamma\cos\gamma\rangle)\}, \end{aligned} \tag{2}$$

$$\begin{aligned} A_Z = k\{&\cos^2\beta\langle\cos^2\Theta\rangle + \sin^2\beta\langle\sin^2\Theta\rangle\langle\sin^2\gamma\rangle \\ &- 2\sin\beta\cos\beta\langle\sin\Theta\cos\Theta\rangle\langle\sin\gamma\rangle\}, \end{aligned} \tag{3}$$

$$\begin{aligned} A_{YZ} = k\{&\langle\sin\varphi\rangle[(\cos^2\beta - \sin^2\beta\langle\sin^2\gamma\rangle)\langle\sin\Theta\cos\Theta\rangle \\ &+ \sin\beta\cos\beta\langle\sin\gamma\rangle(\langle\cos^2\Theta\rangle - \langle\sin^2\Theta\rangle)] \\ &+ \langle\cos\varphi\rangle[\sin^2\beta\langle\sin\Theta\rangle\langle\sin\gamma\cos\gamma\rangle \\ &- \sin\beta\cos\beta\langle\cos\Theta\rangle\langle\cos\gamma\rangle]\}. \end{aligned} \tag{4}$$

The IR beam propagates along the X axis. Averaging of M_Y^2, M_Z^2, and $M_Y M_Z$ should be carried out over all possible orientations of the individual transition moments over the entire sample. This procedure ensures that the molecular orientational distributions through Θ, φ, and γ in a LC sample have been taken into account. For a specific vibration, the polar angle β is assumed to be the same for all the molecules. Using relations (2)–(4), the dichroic ratios $R_{Y,Z}$ and $R_{YZ,Z}$ for a band at a wave number ν can be defined in terms of the absorbances A_Y, A_Z, and A_{YZ} by the equations

$$R_{Y,Z}(\Theta,\varphi,\gamma_\nu,\beta_\nu) = A_Y/A_Z,$$
$$R_{YZ,Z}(\Theta,\varphi,\gamma_\nu,\beta_\nu) = A_{YZ,Z}/A_Z. \tag{5}$$

For a liquid crystalline cell of several micrometers thickness, the absorbance profile $A(\Omega)$ of a particular band (i.e., the dependence of the peak intensity A on the angle of polarization Ω) can be approximated by the equation [15,22]

$$\begin{aligned} A(\Omega) = -\log_{10}[&10^{-A_{\max}} + (10^{-A_{\min}} - 10^{-A_{\max}}) \\ &\times \sin^2(\Omega - \Omega_{\max})], \end{aligned} \tag{6}$$

$\Omega_{\max}$ and $\Omega_{\max}+90°$ are the polarization angles corresponding to the maximal ($A_{\max}$) and minimal ($A_{\min}$) values of the peak intensity, respectively. By fitting Eq. (6) to experimental spectral data the parameters $A_{\max}$, $A_{\min}$, and $\Omega_{\max}$ for an

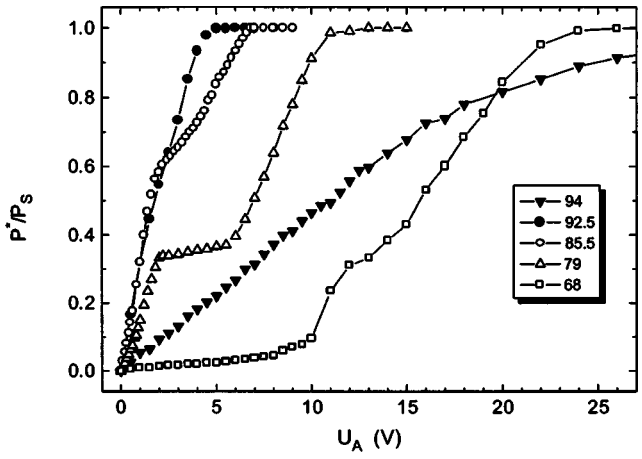

FIG. 3. The voltage dependencies of the normalized macroscopic polarization P^*/P_S for a 6 μm cell of 12OF1M7 at 94 (▼), 92.5 (●), 85.5 (○), 79 (△), and 68 °C (□). The macroscopic polarization P^* was measured by the integral reversed current method [19] using a square wave signal of frequency 52 Hz and amplitude up to 50 V. The saturated value of the polarization, P_S, was temperature dependent. Inset shows symbols and corresponding temperatures (°C).

absorbance profile are determined. The dichroic ratio R is defined in terms of A_{max} and A_{min} by the equation $R=A_{max}/A_{min}$. For a certain band, the absorbances A_Y, A_Z, and A_{YZ} defined by the set of Eqs. (1) can be expressed through A_{max}, A_{min}, and Ω_{max} of the absorbance profile by the equations given in [15,17]:

$$A_Y=A_{min}\cos^2\Omega_{max}+A_{max}\sin^2\Omega_{max}, \tag{7}$$

$$A_Z=A_{min}\sin^2\Omega_{max}+A_{max}\cos^2\Omega_{max}, \tag{8}$$

$$A_{YZ}=(A_{min}-A_{max})\sin\Omega_{max}\cos\Omega_{max}. \tag{9}$$

2. A helical structure

For an ideal helical structure, the molecular distribution as a function of φ is constant for φ in the range of values 0°–360°. This gives $\langle\sin\varphi\rangle=\langle\cos\varphi\rangle=\langle\sin\varphi\cos\varphi\rangle=0$ and $\langle\sin^2\varphi\rangle=0.5$. For an approximate model of a perfect helix in the absence of molecular fluctuations in the tilt plane (the tilt angle Θ is constant for all the molecules), and on assuming free rotation of the molecules about their long axes (the transition moments are uniformly distributed for γ in the range 0° to 360°), we can obtain the following relations from Eqs. (2)–(5):

$$A_{YZ}=0,$$

$$R_{Y,Z}=\frac{A_Y}{A_Z}=\frac{2\sin^2\Theta\cos^2\beta+\cos^2\Theta\sin^2\beta+\sin^2\beta}{4\cos^2\Theta\cos^2\beta+2\sin^2\Theta\sin^2\beta}. \tag{10}$$

Equation (10) is commonly used for describing the IR dichroism of polymers and other anisotropic organic structures [12]. For a FLC helical structure, the molecular distributions through φ, Θ, and γ should be taken into account using Eqs. (2)–(4).

3. The unwound structure

For the field-induced SmC^* phase with unwound structure, the expressions for the absorbances A_Y, A_Z, and A_{YZ} can be obtained using the general equations (2)–(4). For this structure, we assume that the thermal fluctuations in the azimuthal angle φ (Goldstone mode) are suppressed by the electric field and the molecular tilt plane is parallel to the cell substrates. These correspond to $\varphi=90°$ or $-90°$ (depending on the field polarity) for all the molecules. The distribution in the tilt angle Θ is expressed by the averaged functions $\langle\cos^2\Theta\rangle$ and $\langle\sin\Theta\cos\Theta\rangle$ in Eqs. (2)–(4). The equations for the absorbances A_Y, A_Z, and A_{YZ} for the induced SmC^* phase for unwound structure ($\varphi=90°$) are given in [15,17].

For an approximate model of a perfect unwound structure with $\varphi=90°$, a constant value of the tilt angle Θ for all the molecules, and a uniform distribution in the transition moments through γ, the angle Ω_{max}, and dichroic ratio $R=A_{max}/A_{min}$ for a certain band are dependent on its β. For $\beta<\tan^{-1}(2^{1/2})\approx54.44°$, we have $\Omega_{max}=\Theta$ and R can be expressed by the relation [12,17]

$$R=2\cot^2\beta. \tag{11}$$

For $\beta>54.44°$, we have $\Omega_{max}=(\Theta\pm90°)$ and $R=0.5\tan^2\beta$. The molecular arrangement in a field-induced SmC^* phase with unwound structure can be described only approximately by this model. For a biased rotational orientational distribution of molecules through γ, $\Omega_{max}(U_S)$ and $R(U_S)$ for a band are dependent on β and the molecular distributions through Θ and γ, according to Eqs. (2)–(4). The possible azimuthal distributions of the carbonyl transition moments are determined from an analysis of the dichroic data for the phenyl and the carbonyl bands for the unwound SmC^* structure of 12OF1M7. These are given in Sec. IV B.

IV. RESULTS AND DISCUSSION

A. Dichroic parameters as functions of the field

The absorbance profiles for the bands under discussion were deduced from the polarized IR spectra. Figure 4 shows the absorbance profiles for SmC^* at 92.5 °C for helical and unwound structures. The dichroic parameters Ω_{max}, A_{max}, and A_{min} for a certain absorbance profile were determined by fitting Eq. (6) to the experimental data. The reference direction of polarization ($\Omega=0°$) was chosen to coincide with the layer normal in the SmA^* phase at zero field.

The dichroic behavior of the sample as a function of the electric field is illustrated in terms of the voltage dependencies of Ω_{max}, R, A_{max}, and A_{min} for several bands. For a band at a wave number ν, $\Omega_{max\,\nu}$ is a function of the applied voltage U. An angular shift of the absorbance profile, $\Delta\Omega_{max\,\nu}$, is defined as $\Delta\Omega_{max\,\nu}(U)=\Omega_{max\,\nu}(U)-\Omega_{max\,\nu}(0)$. Saturated values of $\Omega_{max\,\nu}$, $\Omega_{max\,\nu}(U_S)$, and $\Delta\Omega_{max\,\nu}$, $\Delta\Omega_{max\,\nu}(U_S)$, are obtained for a saturating voltage U_S such that $\Omega_{max\,\nu}(U)\approx\Omega_{max\,\nu}(U_S)$ for $U\geq U_S$. The determined values of $\Omega_{max}(0)$, $\Omega_{max}(U_S)$, and $\Delta\Omega_{max}(U_S)$ for the studied bands are given in Table I for several temperatures. Below we discuss the dichroic behavior of the phenyl band with increasing field across the LC sample for several temperatures. The dichroic behavior of the carbonyl bands in particular is discussed in Sec. IV A 2.

1. The phenyl band

As the polar angle β_{1604} for 12OF1M7 is rather low ($\beta_{1604}\approx12°$) and the FLC molecules exhibit a distribution through the azimuthal angle γ, the averaged orientation of the transition moments of the phenyl ring C—C stretching vibrations at 1604 cm^{-1} is almost parallel to the molecular long axis. The direction and the degree of preferable orientation of the molecular directors can be characterized by $\Omega_{max\,1604}$ and R_{1604}, respectively. The orientational order parameter $\langle P_2\rangle$ can be found using the equation $\langle P_2\rangle=(R_{1604}-1)/(R_{1604}+2)$.

The voltage dependencies of $\Omega_{max\,1604}$, R_{1604}, $A_{max\,1604}$, and $A_{min\,1604}$ for the phenyl band are shown in Figs. 5 and 6. For all the temperatures studied, $\Omega_{max\,1604}(0)\approx0°$ (see Table I and Fig. 6). It means that for zero field the large axis of the phenyl absorbance profile is almost parallel to the smectic layer normal in the cell, and for the bookshelf structure at zero field the helix in the cell is not distorted and its axis is

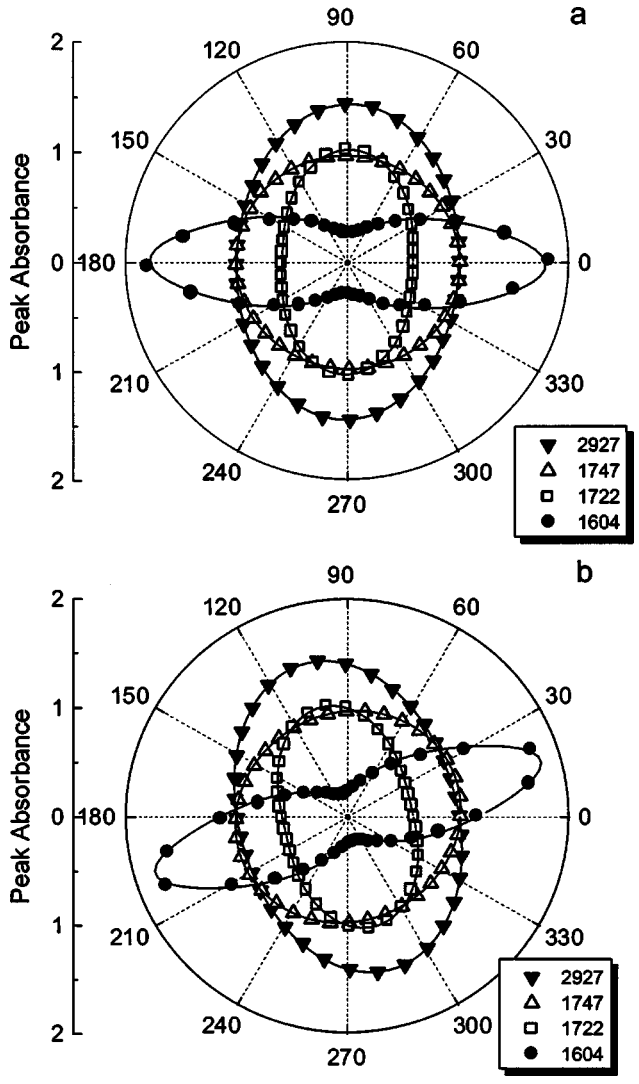

FIG. 4. Polar plots of the absorbance profiles for the phenyl band at 1604 cm^{-1} (●), the carbonyl bands at 1722 cm^{-1} (□) and 1747 cm^{-1} (△), and the methylene band at 2927 cm^{-1} (▼) for the sample in SmC^* at 92.5 °C with helical structure for zero field (a) and electrically unwound structure for a field of ~1.7 V/μm (b). Curves are fits of the function (6) to the experimental data. Wave numbers (cm^{-1}) of the bands are shown in the inset.

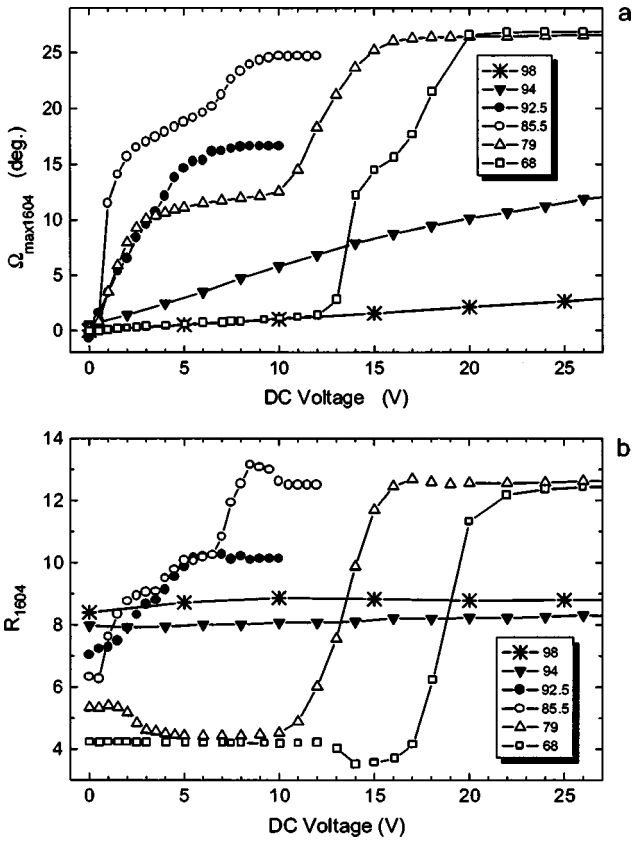

FIG. 5. Ω_{max} (a) and R (b) for the phenyl band at 1604 cm^{-1} vs applied voltage for a 6 μm cell of 12OF1M7 at temperatures 98 (✳), 94 (▼), 92.5 (●), 85.5 (○), 79 (△), and 68 °C (□) shown in the insets.

almost parallel to the smectic layer normal for each phase. As seen from Figs. 5 and 6, the cell exhibits different voltage dependencies of the dichroic parameters of the phenyl band for the various zero-field phase states of the sample at various temperatures.

SmA^*:

For the SmA^* phase at 98 °C, a linear increase in $\Omega_{\max 1604}$ with field is observed [Fig. 5(a)]. The observed behavior arises from the electroclinic effect, which results in a linear dependence of the molecular-induced tilt angle with field. The dichroic ratio R_{1604} [Fig. 5(b)] and the absorbances $A_{\max 1604}$ and $A_{\min 1604}$ (Fig. 6) remain approximately constant in the range of fields from 0 to 10 V/μm studied here. This shows that for measurements at a fixed temperature in the SmA^* phase, the order parameter $\langle P_2 \rangle$, the orientational distribution through Θ, and the resulting averaged parameters $\langle \cos^2 \Theta \rangle$ and $\langle \sin \Theta \cos \Theta \rangle$ do not depend on the field. Note that these parameters do depend on the field for the de Vries type of SmA^* phase [23].

SmC^*_α:

For the SmC^*_α phase at 94 °C, $\Omega_{\max 1604}$ increases monotonically with voltage and exhibits a saturated value of ~15° for fields of ~7.5 V/μm, the increase being linear for a field from 0 to ~2.5 V/μm [Fig. 5(a)]. Such a voltage dependence of $\Omega_{\max 1604}$ is qualitatively similar to that for the optical apparent tilt angle of SmC^*_α [10]. However, it is important to note that the value of R_{1604} has changed relatively little over the voltage range studied [Fig. 5(b)]. An approximately linear increase is found in the dichroic ratio from ~8 (for $U=0$ V) to ~8.5 (for $U=50$ V). This result shows that the averaged molecular distribution through Θ and the orientational order parameter $\langle P_2 \rangle$ for SmC^*_α are almost independent of the electric field. This implies that the SmC^*_α phase is characterized by reduced intra- and interlayer correlations of the molecular tilts as a result of the competition between ferroelectric and antiferroelectric order arising from the fluctuation forces [24]. This results in a reduced interlayer ordering in this phase even for high fields.

SmC^*:

For the SmC^* phase at 92.5 °C, $\Omega_{\max 1604}$ increases rapidly with increasing voltage and saturates at ~16.7° for a comparatively low voltage of ~9 V. Such behavior of

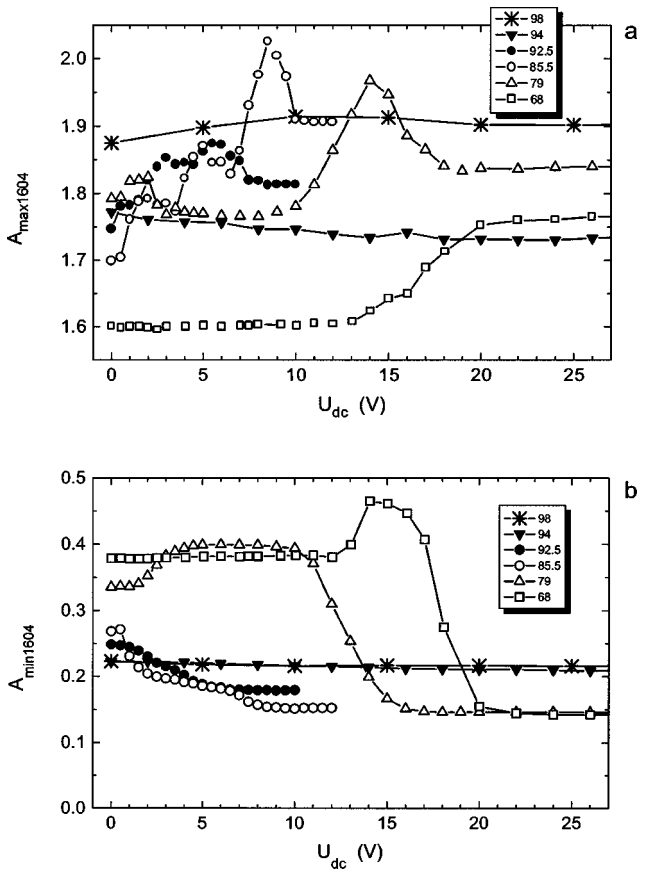

FIG. 6. The voltage dependencies of A_{max} (a) and A_{min} (b) for the phenyl band at 1604 cm^{-1} for the sample at temperatures 98 (✳), 94 (▼), 92.5 (●), 85.5 (○), 79 (△), and 68 °C (□) shown in the insets.

$\Omega_{max\ 1604}$ reflects unwinding of the helix. For zero field, R_{1604} for the SmC^* phase is lower than for the SmA^* and SmC^*_α phases as a result of the presence of the helical structure and comparatively larger molecular tilt angle. In contrast to SmA^* and SmC^*_α, helical unwinding in SmC^* results in a substantial increase in R_{1604} up to ~10 for voltages $U \geqslant 10$ V. The increase in R_{1604} arises mainly from a decrease in $A_{min\ 1604}$; on the contrary the relative increase in $A_{max\ 1604}$ is rather small (see Fig. 6). When the helix is completely unwound, most of the molecules are tilted more or less in the same direction. The reason for a decrease in $A_{min\ 1604}$ with helical unwinding and consequent increase in R_{1604} is that the direction of maximum absorbance ($\Omega_{max\ 1604}$) shifts in the direction of the molecular tilt with unwinding, and consequently the absorbance $A_{min\ 1604}$ (proportional to the average value of the squares of the projections of the phenyl transition moments in the direction normal to the molecular directors in the tilt plane) decreases.

The ferrielectric phase FiLC (SmC^*_{FI3}):

For the cell at 85.5 °C, the observed voltage dependence of $\Omega_{max\ 1604}$ [Fig. 5(a)] is typical of the state of a ferrielectric FiLC phase (SmC^*_{FI3}) at zero field [17]. For the low voltage range $0 < U < 2$ V, a rapid increase in both $\Omega_{max\ 1604}$ (from 0° to ~65% of the saturated value of $\Omega_{max\ 1604}$ for this temperature) and R_{1604} by a factor of 1.5 is observed. These

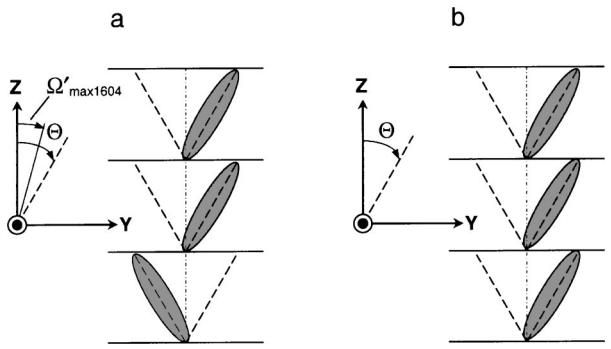

FIG. 7. Schematic illustration of the molecular orientation in unwound structures for SmC^*_γ (SmC^*_{FI1}) (a) and SmC^* (b). The (X,Y,Z) frame is the same as in Fig. 1, Θ is the molecular tilt angle, and the angle $\Omega'_{max\ 1604}$ for SmC^*_γ is described in the text.

large increases arise from a rapid deformation of the helix with increasing field. The increase in R_{1604} arises again mainly from a decrease in A_{min} and a slight increase in A_{max} (Fig. 6), as for the SmC^* phase. For the range $2 < U < 6$ V, the increase in $\Omega_{max\ 1604}$ and R_{1604} has a lower rate than for the lower voltage range (Fig. 5). The state of a comparatively slow increase in $\Omega_{max\ 1604}$ and R_{1604} with field is connected with a continuous phase transition to the field-induced SmC^* phase through a variety of intermediate induced subphases and further distortion of the helix [17]. At the final stage of the field-induced process, both $\Omega_{max\ 1604}$ and R_{1604} demonstrate considerable increases in their values for the voltage range $6 < U < 10$ V. A saturation in their values for $U \geqslant 10$ V is reached and this state corresponds to the field-induced SmC^* phase with unwound structure. We note here that in contrast with the results obtained for a cell with ZnSe windows [17], R_{1604} for the cell with CaF_2 windows is substantially higher. In this case the large decrease in R_{1604} for high fields (arising from the striped-bookshelf structure) reported in Ref. [17] was not repeated; only a small decrease in R_{1604} by ~5% from its maximum value is found for a voltage in the range 9–10 V [Fig. 5(b)]. From this result, we conclude that the layer structure in a cell with CaF_2 substrates remains bookshelf-like for the entire range of the bias fields applied across the cell. We also note that the voltage dependence of $\Omega_{max\ 1604}$ [Fig. 5(a)] is qualitatively similar to the voltage dependence of the macroscopic spontaneous polarization for the temperature range corresponding to the FiLC (SmC^*_{FI3}) subphase (see Fig. 3 and Refs. [8,17]).

SmC^*_γ (*SmC^*_{FI1}*):

Application of a low field of ~0.5 V/μm across the cell in the SmC^*_γ phase at 79 °C results in a rapid and almost linear increase in $\Omega_{max\ 1604}$ from ~0° to ~11° [Fig. 5(a)] and a decrease in R_{1604} from 5.3 to 4.4 [Fig. 5(b)] for U from 0 to 3 V. A decrease in R_{1604} with increase in bias can occur from the combined effects of (a) helical unwinding and (b) the directors in the layers of the unit cell becoming planar with the field (see Fig. 7). Note that the distortion angles by which the directors are nonplanar in ferrielectric phases of 12OF1M7 have been found to be rather small [4,9], i.e., the distortion from the Ising model is small. Helical unwinding is therefore the main cause of a reduction in R_{1604} for the

voltage range 0 to 4 V for SmC^*_γ. The reason that R_{1604} for SmC^*_γ decreases with helical unwinding, unlike for the SmC^* and FiLC phases (where it increases monotonically), is that the direction of maximum absorbance in the SmC^*_γ phase does not shift very significantly with increase in the bias field, as it does in the SmC^* and FiLC phases. The absorbance along the normal direction $A_{\min 1604}$ for the SmC^*_γ phase will therefore increase (Fig. 6) with total helical unwinding for the planar molecular orientation shown in Fig. 7 and consequently R_{1604} will decrease [Fig. 5(b)]. The presence of SmC^*_γ with unwound structure for voltages in the range 4–10 V is characterized by the minimal value of R_{1604} and a quasistable value of $\Omega_{\max 1604}$. On increasing the voltage from 10 to ~16 V across the cell, a phase transition from SmC^*_γ to the field-induced SmC^* phase is observed. In the dichroic properties, this is accompanied by a substantial increase in both $\Omega_{\max 1604}$ and R_{1604}. The latter increases by a factor of 3, caused mainly by a decrease in $A_{\min 1604}$ (Fig. 6) for the reasons given under the section for the SmC^* phase.

For $U=8$ V, $\Omega_{\max 1604}$ is about 45% of its saturated value $\Omega_{\max 1604}(20\text{ V})=26.5°$. This result is in good agreement with the model of the molecular orientations for the unwound structures of SmC^*_γ and SmC^* shown in Fig. 7. For both phases, in the unwound case, the molecules are parallel to the surfaces of the substrates in the (Y,Z) plane. For SmC^*_γ with a periodicity of three layers, the molecules in two consecutive layers are tilted clockwise with an angle of Θ to the smectic layer normal, whereas in the third layer the directors are tilted by the same angle counter-clockwise [Fig. 7(a)]. For the unwound SmC^* structure, all the molecules are parallel to each other [Fig. 7(b)]. The polarization angle $\Omega'_{\max}$, which corresponds to the maximal absorbance of the phenyl band at 1604 cm^{-1} for the structure shown in Fig. 7(a), can be found from the equation $3\tan(2\Omega'_{\max})=\tan(2\Theta)$ for $\beta_{1604}\cong 0°$. For the observed value of $\Theta \approx \Omega_{\max 1604}(20\text{ V})=26.5°$ at a temperature of 79 °C, we obtain $\Omega'_{\max}\approx 11.9°$. This is in good agreement with the experimental value of $\Omega_{\max 1604}(12\text{ V})\approx 12°$.

SmC^*_A:

The LC sample at 68 °C is in its helical SmC^*_A state for voltages in the range 0 to a threshold of ~12 V. For this voltage range, $\Omega_{\max 1604}$ exhibits a very slow linear increase [Fig. 5(a)] while R_{1604} does not change with voltage and remains low [Fig. 5(b)]. The slope for the curve $\Omega_{\max 1604}(U)$ is exactly similar to that for the voltage dependence of $\Omega_{\max 1604}$ for the SmA^* phase at 98 °C [Fig. 5(a)]. These results show that for SmC^*_A as well as for SmA^*, low electric fields cause only a small angular shift of the phenyl absorbance profile. For $12<U<15$ V, the induced phase transition from SmC^*_A to SmC^*_γ and simultaneous helical unwinding take place. This is reflected in terms of the angular shift in $\Omega_{\max 1604}$ and a decrease in R_{1604} after the change from the nonplanar to the planar molecular orientation has occurred. The likely reason for the unwinding of the helix at 68 °C to occur for a significantly larger voltage is that the helical pitch for SmC^*_A (zero field) is much shorter than for the other phases. For $16\leqslant U\leqslant 25$ V, the induced phase transition from SmC^*_γ to SmC^* is observed. The helix of the latter is already unwound as the field is too large. This leads to a substantial increase in both $\Omega_{\max 1604}$ and R_{1604} and their saturation occurs for $U_S\approx 25$ V.

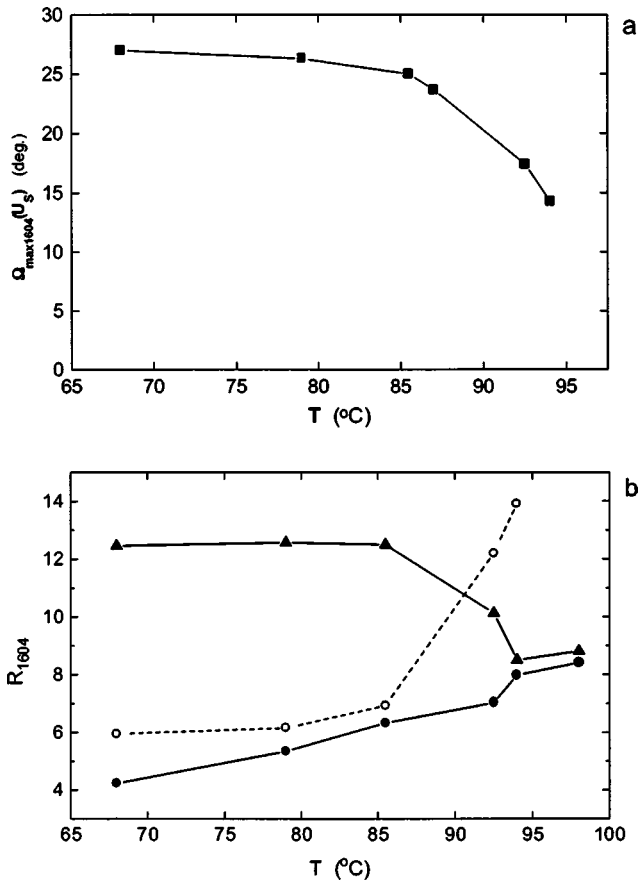

FIG. 8. The temperature dependencies of (a) $\Omega_{\max 1604}(U_S)$ for unwound structure (■); (b) $R_{1604}(0)$ for helical structure at zero field (●) and $R_{1604}(U_S)$ for unwound structure (▲). Sample: 6 μm cell of 12OF1M7. Solid symbols correspond to fits of the experimental data using Eq. (6). Open circles in (b) show values of $R_{Z,Y}$ calculated using Eq. (10) for $\beta_{1604}=15°$ and $\Theta=\Omega_{\max 1604}(U_S)$. (Values of U_S are given in Table I. Lines interconnect adjacent data points.)

Temperature dependences of the molecular apparent tilt and the dichroic ratio:

The polarization angle $\Omega_{\max 1604}(U_S)$ corresponding to the maximum absorbance of the phenyl profile for the saturating voltage is related to the molecular apparent tilt angle, since $\beta_{1604}\approx 12°$ and the average orientation of the phenyl transition moment is almost parallel to the long molecular axis. The temperature dependence of $\Omega_{\max 1604}(U_S)$ is shown in Fig. 8. For a decrease in temperature from 94 to 85.5 °C, a comparatively rapid increase in the saturated angular shift of the phenyl profile $\Delta\Omega_{\max 1604}(U_S)$ from 14.3° to 25° is observed. However, for the range 85.5–68 °C, the rate of increase in $\Omega_{\max 1604}(U_S)$ with a decrease in temperature is substantially lower. Note that for a certain temperature $\Omega_{\max 1604}(U_S)$ is found to be close to the molecular apparent tilt angle determined using polarizing microscopy, as is typical of cells of FLCs and AFLCs [13–15].

As seen from Figs. 5(b) and 8(b), the dichroic ratio R_{1604} (as well as the related order parameter $\langle P_2 \rangle$) for helical and unwound structures in the LC sample is temperature dependent. On cooling the sample, $R_{1604}(0)$ and $\langle P_2 \rangle$ decrease with decrease in temperature in the temperature range studied. For SmA^*, the dichroic ratio of the phenyl band is determined mainly by the thermal fluctuations of the molecular orientations through the angle Θ, since $\beta_{1604} \approx 15°$ is rather small and the experimental value of $R_{1604}(0) \approx 8.4$ cannot be explained in terms of the rotational distribution through γ only. For the tilted phases, $\Omega_{\max 1604}(0) \approx 0°$ and $R_{1604}(0) = R_{Z,Y}$. For the helical molecular distribution through φ, $R_{1604}(0)$ is dependent on β_{1604}, the molecular tilt angle $\Theta_0 = \Omega_{\max 1604}(U_S)$, and the molecular distribution through Θ. The latter is connected with the soft mode. For an ideal helical structure and a small enough value of β_{1604}, Eq. (10) reflects a tendency for a decrease in $R_{1604}(0)$ on increasing the molecular tilt angle $\Theta_0 = \Omega_{\max 1604}(U_S)$ when the sample is cooled at zero field [open circles in Fig. 8(b)]. However, the approximate equation (10) gives a significantly larger value of $R_{1604}(0)$ in comparison with the experimental results, as it does not take into account the molecular fluctuations in the tilt plane (through Θ) as well as out of the tilt plane (through φ), which do exist as the soft and the Goldstone modes, respectively, for zero field. The discrepancy between the experimental results for the helical cell and the values of $R_{Z,Y}$ estimated using Eq. (10) is especially pronounced for the temperature intervals of the SmC^*_α and SmC^* phases. This can be explained by relatively large fluctuations in the tilt angle and the reduced order parameter at higher temperatures.

For the unwound structure, $R_{1604}(U_S)$ increases with decreasing temperature from 94 to 85.5 °C and remains almost constant for temperatures in the range of 85.5 to 68 °C [Fig. 8(b)]. For the approximate model of the perfect unwound structure and the order parameter of unity, Eq. (11) gives an upper limiting value of $R_{1604} \approx 28$ for $\beta_{1604} = 15°$. This is substantially higher than the experimental values of $R_{1604}(U_S)$ for the studied cell. Molecular orientational fluctuations may still occur even when the structure is electrically unwound. This may be the main reason for the order parameter to be much lower than unity in the smectic phases. A reduction of $R_{1604}(U_S)$ in the experiment can also result from the boundary layers in close proximity to the substrates, where the molecules may lie parallel to the rubbing direction, i.e., in a different direction from the molecules in the bulk of the cell.

2. The carbonyl and methylene bands

The dichroic behavior of the carbonyl bands at 1722 and 1747 cm^{-1} and the methylene band at 2927 cm^{-1} with bias field is illustrated in Figs. 9–11. These bands exhibit substantially lower dichroism than is observed for the phenyl band at 1604 cm^{-1}, mainly because of the differences in the polar angles β for the transition moments. In particular, the values of $\beta_{1722} \approx 63.5°$ and $\beta_{1747} \approx 53.5°$ are determined from the IR dichroic data in Sec. IV B. For a helical structure at zero field and for the field-induced SmC^* phase with unwound

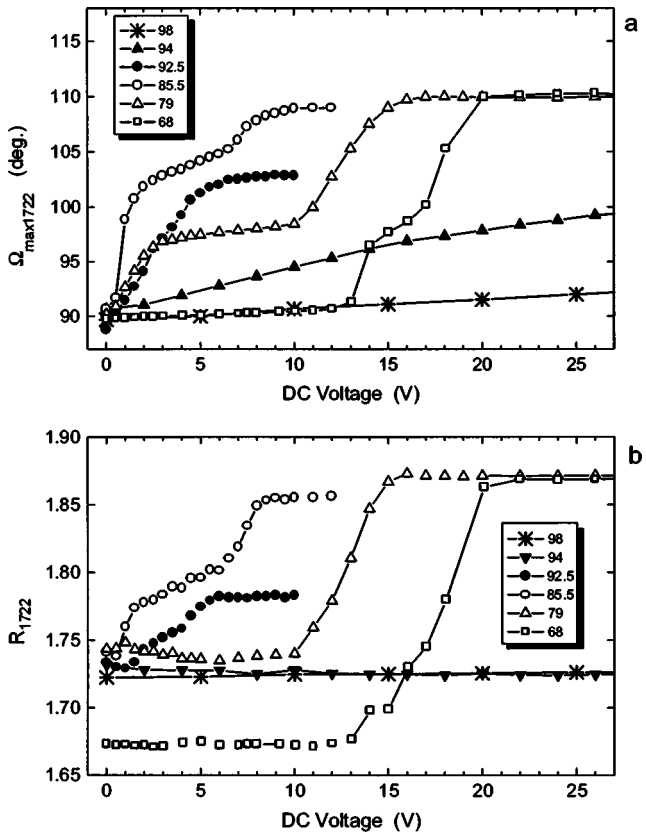

FIG. 9. $\Omega_{\max}$ (a) and R (b) for the carbonyl band at 1722 cm^{-1} vs applied voltage for a 6 μm cell of 12OF1M7 at temperatures 98 (✳), 94 (▼), 92.5 (●), 85.5 (○), 79 (△), and 68 °C (□) shown in the insets.

structure, the experimental values of R_{1722} and R_{1747} are in qualitative agreement with those estimated for the dichroic ratios obtained using Eqs. (10) and (16), respectively, by substituting Θ equal to $\Omega_{\max 1604}(U_S)$ (see Table I).

For the bands at 1722 and 2927 cm^{-1}, $\Omega_{\max}(0)$ values are found to be close to 90° [see Figs. 4, 9(a), and 11(a) and Table I). This is typical of a ''chiral'' carbonyl and the methylene bands of chiral FLC materials [13,15]. As can be seen from Figs. 5(a), 9(a), and 11(a), the voltage dependencies of the angular shifts $\Delta\Omega_{\max}(U)$ for the bands at 1722 and 2927 cm^{-1} are similar to that for the phenyl band at 1604 cm^{-1}. This result can be explained by the properties of the molecular orientational distribution functions of a chiral smectic liquid crystalline sample, which are related to the parameters of the absorbance profiles of the various dichroic bands for which the polar angles β are substantially different from the critical angle of ~54.44° [17]. The relationships can be analyzed using Eqs. (2)–(4) and (7)–(9). If the degree of rotational biasing is small, the relative angular shifts of the absorbance profiles of the various bands are dependent on changes in the molecular distribution through φ. This distribution is affected by the field-induced processes of phase transitions and helical unwinding. Furthermore, the voltage dependencies of the relative angular shifts of the profiles $\Delta\Omega_{\max}(U)/\Delta\Omega_{\max}(U_S)$ for the dichroic bands at 1604, 1722, and 2927 cm^{-1} are found to be qualitatively similar to the

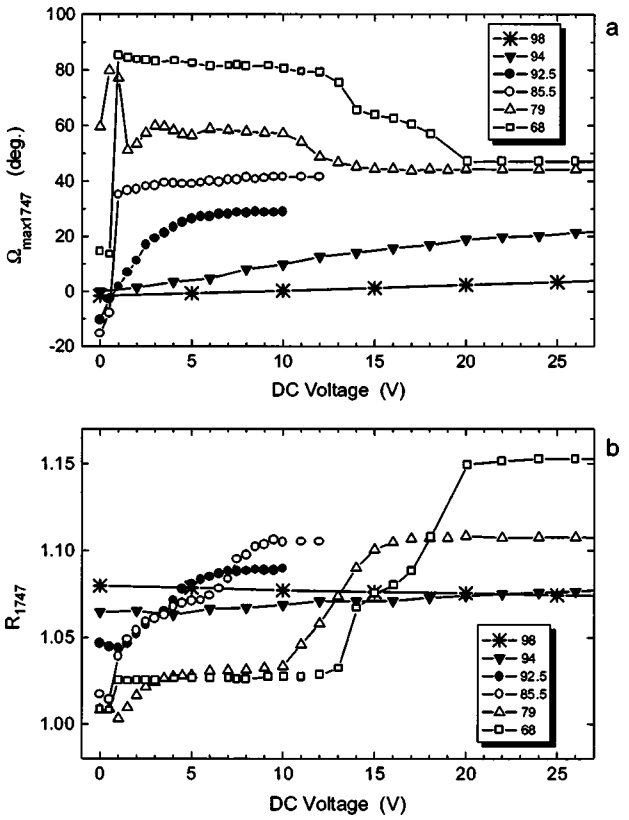

FIG. 10. Ω_{max} (a) and R (b) for the carbonyl band at 1747 cm^{-1} vs applied voltage for a 6 μm cell of 12OF1M7 at temperatures 98 (✳), 94 (▼), 92.5 (●), 85.5 (○), 79 (△), and 68 °C (□) shown in the insets.

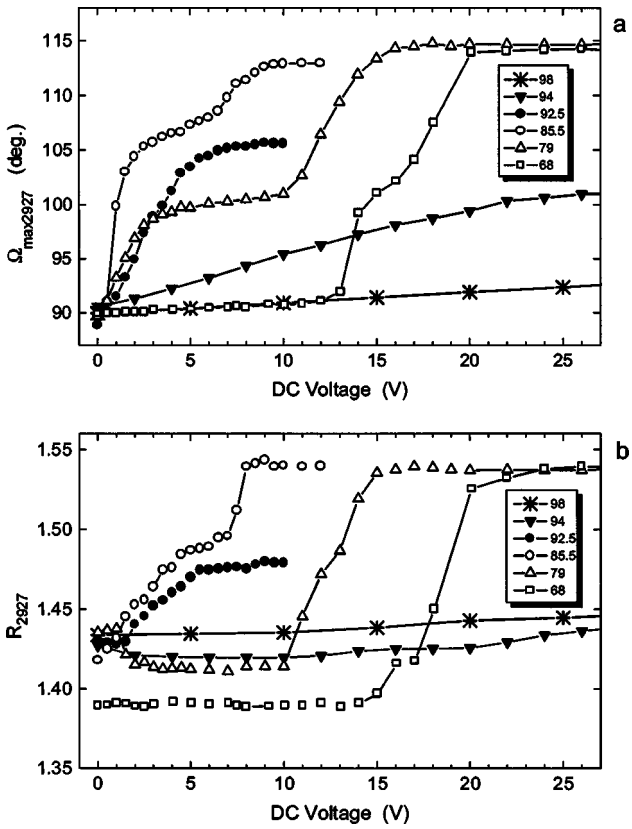

FIG. 11. Ω_{max} (a) and R (b) for the methylene band at 2927 cm^{-1} vs applied voltage for a 6 μm cell of 12OF1M7 at temperatures 98 (✳), 94 (▼), 92.5 (●), 85.5 (○), 79 (△), and 68 °C (□) shown in the insets.

voltage dependence of P^*/P_S (Fig. 3). This similarity follows from the fact that both the IR dichroic parameters and the effective macroscopic polarization of a chiral smectic liquid crystal possessing head-and-tail equivalence are dependent on the orientational distributions. These distributions, particularly in φ, can be altered by the external field.

However, for the tilted phases at temperatures of 94, 92.5, 85.5, 79, and 68 °C, the absorbance profiles of the carbonyl and methylene bands are asymmetric with respect to the major axis of the phenyl profile. This is reflected in the substantial differences in the saturated values of $\Delta\Omega_{max}(U_S)$ for the various bands (Table I). For example, at temperatures 94 and 68 °C, the values of $\Delta\Omega_{max}(U_S)$ for the bands at 1604 and 1722 cm^{-1} differ by 3.6° and 8.8°, respectively. This result is direct evidence for the existence of a biased rotational orientational distribution of the molecules around their long axes [13]. The dichroic behavior of the band at 2927 cm^{-1} is related to the molecular structure discussed in Sec. III A. A noncollinear orientation of the two aliphatic tails in a molecule with $\beta_{2927} \sim 60° - 70°$ and the orientational distributions of the molecules in a LC sample give rise to a low R_{2927} in comparison with R_{1604}. The low dichroism of the methylene bands has already been reported for a number of FLCs [13–15].

The "core" carbonyl band at 1747 cm^{-1} exhibits very low dichroism, $1 < R_{1747} < 1.15$, for the temperatures studied for both zero and higher fields across the cell [Fig. 10(b)]. This result is in good agreement with R estimated using Eqs. (10) and (11) for $\beta_{1747} \approx 53.5°$ (determined in Sec. IV B). This value of β_{1747} is close to the critical angle $\beta = \tan^{-1}(2^{1/2}) \approx 54.44°$ for which $R = 1$ for both the helical and unwound structures in accordance with Eqs. (10) and (11).

B. Molecular distribution through the azimuthal angle γ

We determine the orientational distributions of the C═O vibrational transition moments in terms of the azimuthal angle γ from the observed dichroic data for the phenyl and carbonyl bands at 1604, 1722, and 1747 cm^{-1} for several temperatures in the range of 68–94 °C. The field-induced SmC^* phase with unwound structure is investigated. A numerical analysis of the dichroic parameters for a set of three bands is carried out using the improved procedure developed in [17]. For a band of wave number ν, we consider a set of two equations (5) for a fixed temperature. The dichroic ratios $R_{Y,Z}$ and $R_{YZ,Z}$ are expressed as functions of the angles Θ, φ, γ_ν, and β_ν using the set of equations (2)–(4) for $\varphi = -90°$. This corresponds to the unwound SmC^* structure. The numerical values of $R_{Y,Z}$ and $R_{YZ,Z}$ are determined in terms of the values of A_Y, A_Z, and A_{YZ} that are obtained from Eqs. (7)–(9) using the fitted parameters $\Omega_{\max \nu}$, $A_{\max \nu}$, and $A_{\min \nu}$ of the profiles for $U = U_S$. The molecular orientational distribution through the tilt angle Θ is described by

TABLE III. The azimuthal parameters $\langle \sin\gamma \rangle$, $\langle \sin^2\gamma \rangle$, a_1, a_2, and γ_0 of the transition moments of the carbonyl vibrations at 1722 and 1747 cm^{-1} for the unwound SmC^* structure at several temperatures.

T (°C)	Band (cm^{-1})	$\langle \sin\gamma \rangle$	$\langle \sin^2\gamma \rangle$	a_1	a_2	γ_0 (deg)
94	1722	−0.028	0.502	0.017	−0.003	−31.3
	1747	−0.013	0.504	0.017	−0.003	−14.7
92.5	1722	−0.033	0.501	0.018	−0.002	−35.4
	1747	−0.015	0.503	0.018	−0.002	−15.5
85.5	1722	−0.049	0.4999	0.022	−0.002	−45.3
	1747	−0.022	0.502	0.022	−0.002	−18.8
79	1722	−0.057	0.4999	0.024	−0.002	−48.7
	1747	−0.024	0.503	0.024	−0.002	−18.4
68	1722	−0.071	0.501	0.031	0.01	−47.0
	1747	−0.037	0.489	0.031	0.01	−22.5

the averages $\langle \cos^2\Theta \rangle$ and $\langle \sin\Theta\cos\Theta \rangle$. The azimuthal distribution of the molecules in terms of γ is described by the function given by Jang *et al.* [15]

$$f(\gamma) = 1/(2\pi) + a_1 \cos(\gamma - \gamma_0) + a_2 \cos 2(\gamma - \gamma_0), \tag{12}$$

where γ_0 is the biasing angle, and a_1 and a_2 are the biasing coefficients. The averaged functions $\langle \sin\gamma \rangle$ and $\langle \sin^2\gamma \rangle$ can be found as $\langle \sin\gamma \rangle = a_1\pi \sin\gamma_0$, $\langle \sin^2\gamma \rangle = 0.5(1 - \pi a_2 \cos 2\gamma_0)$.

To determine the unknown parameters β, $\langle \sin\gamma \rangle$, and $\langle \sin^2\gamma \rangle$ for each band, and the director parameters $\langle \cos^2\Theta \rangle$ and $\langle \sin\Theta\cos\Theta \rangle$ for the unwound SmC^* structure, a system of six equations of type (5) for the bands at 1604, 1722, and 1747 cm^{-1} for a particular temperature is solved in several steps using the package MATHCAD 2000 PRO. At a first step, we set $\langle \sin^2\gamma \rangle = 0.5$ for the various bands and also set $\beta_{1604} = 0°$. The initial values of $\beta_{1722} = 76°$ and $\beta_{1747} = 68°$ are taken from the results for the polar angles of the two C═O bonds (Sec. III A). The parameters β and $\langle \sin\gamma \rangle$ for the two carbonyl bands and the parameters $\langle \cos^2\Theta \rangle$ and $\langle \sin\Theta\cos\Theta \rangle$ so obtained are used as their initial values for the next step. In the second step, β, $\langle \sin\gamma \rangle$, and $\langle \sin^2\gamma \rangle$ for the 1722, 1747, and 1604 cm^{-1} bands and $\langle \cos^2\Theta \rangle$ and $\langle \sin\Theta\cos\Theta \rangle$ are varied for the set of equations. Stable solutions are obtained for the polar angles to have values $\beta_{1604} = 11.9° \pm 0.1°$, $\beta_{1722} = 63.5° \pm 0.2°$, and $\beta_{1747} = 53.5° \pm 0.2°$, for the temperature range investigated. At the next step, $\langle \sin\gamma \rangle$ and $\langle \sin^2\gamma \rangle$ for the bands for each temperature were determined by solving the set of equations (5) for fixed values $\beta_{1604} = 12°$, $\beta_{1722} = 63.5°$, and $\beta_{1747} = 53.5°$. Finally, the biasing parameters $\gamma_{0\nu}$, a_1, and a_2 were determined from $\langle \sin\gamma \rangle$ and $\langle \sin^2\gamma \rangle$. The coefficients a_1 and a_2 are assumed to be the same for the various bands. This assumption can be justified on the basis of a sufficiently rigid molecular core. The results obtained for the carbonyl bands are listed in Table III. We find that the fitted values of β_{1722} and β_{1747} are ~14° lower than the polar angles for the two C═O bonds (Sec. III A). This can be explained by the possible existence of an angle of ~10°–20° between the C═O stretching transition moment and the carbonyl bond [12]. We remark that the determined values of β_{1722} and β_{1747} are lower by ~4° than the values reported earlier in [17] for the same compound. The values determined here are regarded to be more accurate since higher dichroism for the phenyl band is achieved for the bookshelf structure for a cell with CaF_2 windows. This is different from the striped bookshelf structure observed previously in a cell with ZnSe windows [17].

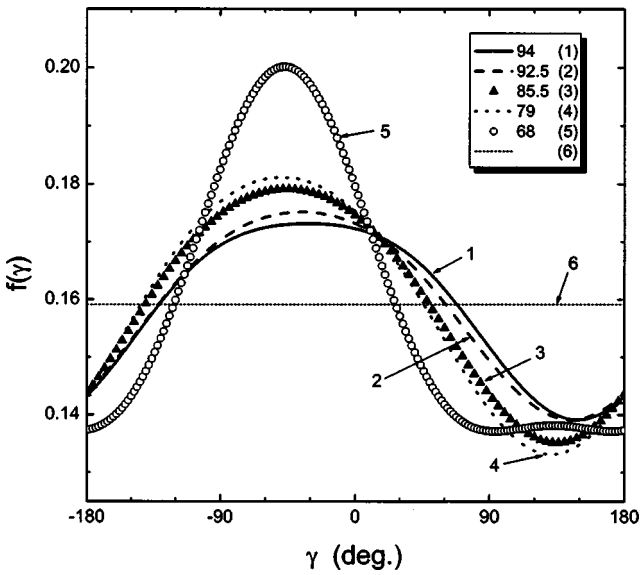

FIG. 12. Possible azimuthal distributions $f(\gamma)$ of the transition moments of the carbonyl vibrations at 1722 cm^{-1} for unwound SmC^* structure 12OF1M7 at temperatures 94 (1), 92.5 (2), 85.5 (3), 79 (4), and 68 °C (5). Curves 1–5 in polar plots correspond to the molecules with the "chiral" C_8H_{17} tail oriented toward the reader. For the molecules with the C_8H_{17} tail away from the reader, the distributions correspond to functions $f(-\gamma)$ for various temperatures. For comparison, curve 6 shows the distribution $f(\gamma) = 1/(2\pi)$ for zero degree of biasing ($a_1 = a_2 = 0$).

Figure 12 shows the azimuthal distributions $f(\gamma)$ of the transition moments for the "chiral" carbonyl band at 1722 cm^{-1} for the field-induced unwound SmC^* phase at several temperatures. The angle γ_o gives the most probable azimuthal orientation of the transition moment for a certain band. Figure 13 illustrates the orientations of the "chiral" C═O groups for head-and-tail equivalent molecules with the most probable azimuthal orientations of the 1722 cm^{-1} transition moments. Note that both angles γ_o and $(180° - \gamma_o)$ correspond to the determined values of $\langle \sin\gamma \rangle$ and $\langle \sin^2\gamma \rangle$. As seen from Table III and Fig. 12, the molecular distribution $f(\gamma)$ is temperature dependent. With a decrease in temperature, the absolute value of the biasing angle γ_0 for both carbonyl bands increases. Figure 14 shows the possible azimuthal distribution functions $f(\gamma)$ of the "chiral" C═O groups for the unwound SmC^* structure at 92.5 °C. In agreement with the analysis reported in Refs. [13–15], an effective spontaneous polarization appears along the C_2 symmetry axis due to the existence of the head-and-tail equivalence and the biasing in the azimuthal orientational distribution of the FLCs molecules. For the unwound SmC^* structure, the

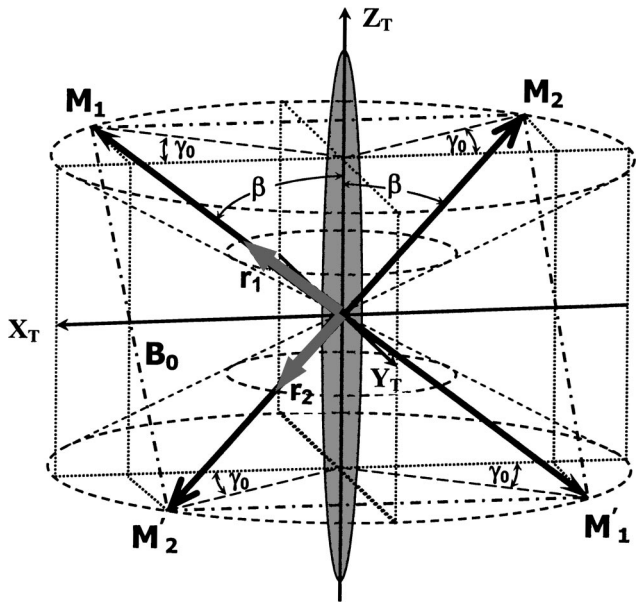

FIG. 13. Schematic illustration of the orientations of the ''chiral'' C═O groups for the head-and-tail equivalent molecules with 1722 cm^{-1} transition moments $\mathbf{M}_1$ and $\mathbf{M}_2$ characterized by the most probable azimuthal angles of γ_o and $(180°-\gamma_o)$, respectively. The frame (X_T, Y_T, Z_T) is related to the molecular tilt plane (Fig. 1). For simplicity, the C—O director (vector $\mathbf{r}$) is assumed to be collinear with $\mathbf{M}$. In this case, $\mathbf{r}_1$ and $\mathbf{r}_2$ are characterized by the azimuthal angles γ_0 and $-\gamma_0$, respectively. The vectors $\mathbf{r}_1$, $\mathbf{M}_1$, and $\mathbf{r}_2$, $\mathbf{M}_2$ correspond to molecules with the C_8H_{17} tail oriented up (positive direction of the Z_T axis) and down, respectively. The effective polarization appears along the X_T axis, which for an unwound structure is normal to the substrates.

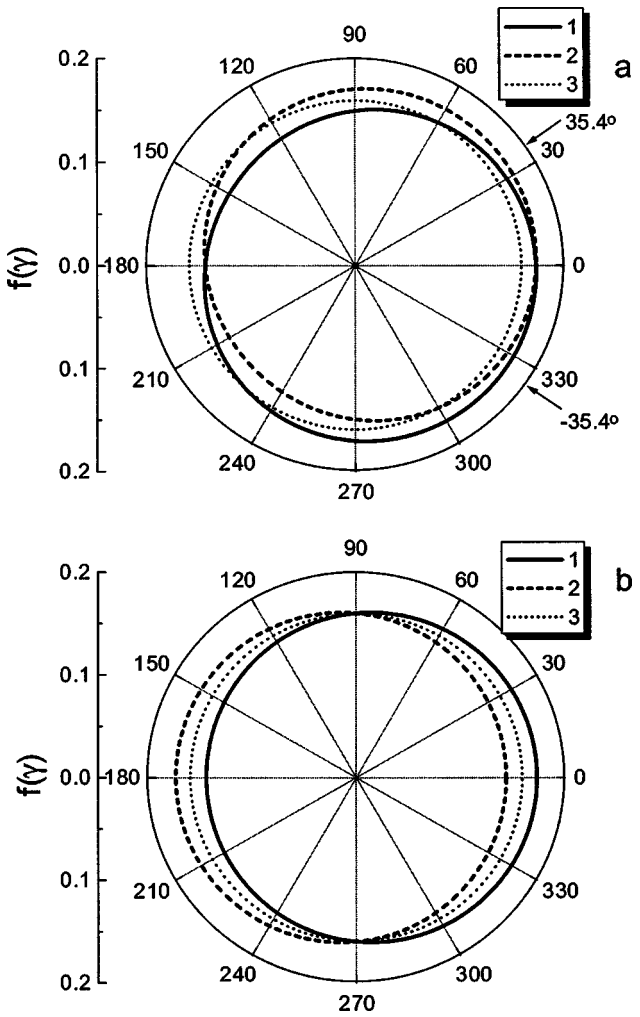

FIG. 14. Possible distributions $f(\gamma)$ of the ''chiral'' carbonyl groups for unwound SmC^* structure at 92.5 °C in polar plots. (a) $f(\gamma)$ and $f(-\gamma)$ are the distributions for molecules with the C_8H_{17} tail oriented toward the reader (solid curve 1) and away from the reader (dashed curve 2), respectively. (b) Solid curve 1 shows the average distribution $[f(\gamma)+f(-\gamma)]/2$ for all molecules for a given polarity of the applied field. The resultant polarization is negative. Dashed curve 2 shows the average distribution of the ''chiral'' C═O groups $[f(\gamma-\pi)+f(-\gamma-\pi)]/2$ for the opposite field. (Dotted curves 3 show the function $f(\gamma)=(2\pi)^{-1}$ in the absence of azimuthal biasing.)

C_2 axis is parallel to the X axis, which coincides with the X_T axis for $\varphi=\pm 90°$ (see Fig. 1).

A decrease in temperature from 94 to 68 °C results in γ_{o1722} varying from $-31.3°$ to $-47°$ and γ_{o1747} varying from $-14.7°$ to $-22.5°$. A substantial increase (approximately by a factor of 2) in the parameter a_1 is also observed with a decrease in temperature. This reflects an increase in the degree of polar azimuthal biasing of the C═O groups. In the temperature range from 94 to 79 °C, corresponding to the ferro- and ferrielectric phases at zero field, the quadrupolar biasing is found to be low. The absolute value of the parameter a_2, which characterizes the second Fourier component in the function (12), is lower than a_1 by a factor that varies from 6 to 12. However, for a temperature of 68 °C (corresponding to SmC_A^* for zero field), the quadrupolar biasing is rather important as a_2 is only a factor of ~ 3 lower than a_1. This may imply an important relationship between the quadrupolar rotational biasing and the degree of anticlinic ordering in the SmC_A^* phase even in the absence of dc bias. The results obtained quantitatively yield the differences in the molecular rotational orientational distributions for the field-induced SmC^* phase for various temperatures that correspond to the different phases of a chiral smectic liquid crystal.

V. CONCLUSIONS

The IR dichroic behavior of a homogeneously aligned cell of a chiral smectic liquid crystal 12OF1M7 under an external electric field is found to be strongly dependent on the phase state at zero field. The observed voltage dependencies of the polarization angle of maximal absorbance and the dichroic ratio of the characteristic bands are interpreted in terms of the phase structure, the molecular orientational distributions, and the polar angles of the transition moments. The dichroic ratio of the phenyl band R_{1604} is found to be lowest for the SmC_A^* and SmC_γ^* phases and highest for the corresponding field-induced SmC^* phases with unwound structure. For the SmC^* and FiLC phases, R_{1604} increases on helical unwind-

ing whereas for the SmC_A^* and SmC_γ^* phases R_{1604} shows a minimum for the planar unwound structure and then increases with the induced phase transition to SmC^*. This is explained in terms of the differences in the director distributions and the dependence of the polarization angle of maximum absorbance on the bias field in these phases.

For the field-induced SmC^* unwound structure, the rotational orientational distribution of the carbonyl transition moments exhibits a temperature-dependent bias. The angle of biasing for the chiral carbonyl band is found to be greater than that for the core carbonyl band by at least a factor of 2. The degree of biasing and the shift in the most probable azimuthal angle increase with decrease in temperature. For temperatures that correspond to the ferro- and ferrielectric phases (at zero field), polar biasing is found to be predominant. In contrast, for lower temperatures, the contributions of the components of the polar and quadrupolar biasing have been found to be comparable to each other. The quadrupolar biasing coefficient is found to reverse its sign and increase by a factor of 5 for a decrease in temperature that corresponds to the SmC_γ^* and SmC_A^* phases at zero field.

ACKNOWLEDGMENTS

The work was supported by the EU Grant SAMPA and the Ireland Grant SFI G20021-2003. We thank O. E. Panarina for measurements of the macroscopic spontaneous polarization and Professor A. Fukuda for useful discussions.

[1] P. Mach, R. Pindak, A.-M. Levelut, P. Barois, H. T. Nguyen, C. C. Huang, and L. Furenlid, Phys. Rev. Lett. **81**, 1015 (1998).
[2] P. M. Johnson, D. A. Olson, S. Pankratz, H. T. Nguyen, J. W. Goodby, M. Hird, and C. C. Huang, Phys. Rev. Lett. **84**, 4870 (2000).
[3] X. F. Han, D. A. Olson, A. Cady, D. R. Link, N. A. Clark, and C. C. Huang, Phys. Rev. E **66**, 040701(R) (2002).
[4] N. M. Shtykov, J. K. Vij, and H. T. Nguyen, Phys. Rev. E **63**, 051708 (2001).
[5] V. P. Panov, J. K. Vij, N. M. Shtykov, S. S. Seomum, D. D. Parghi, M. Hird, and J. W. Goodby, Phys. Rev. E **67**, 021702 (2003).
[6] K. Itoh, M. Kabe, K. Miyachi, Y. Takanishi, K. Ishikawa, H. Takezoe, and A. Fukuda, J. Mater. Chem. **7**, 407 (1997).
[7] T. Matsumoto, A. Fukuda, M. Johno, Y. Motoyama, T. Yui, S. S. Seomun, and M. Yamashita, J. Mater. Chem. **9**, 2051 (1999).
[8] Yu. P. Panarin, O. Kalinovskaya, J. K. Vij, and J. W. Goodby, Phys. Rev. E **55**, 4345 (1997).
[9] N. M. Shtykov, J. K. Vij, R. A. Lewis, M. Hird, and J. W. Goodby, Liq. Cryst. **28**, 1699 (2001).
[10] A. Fukuda, Y. Takanishi, T. Isozaki, K. Ishikawa, and H. Takezoe, J. Mater. Chem. **4**(7), 997 (1994).
[11] S. T. Lagerwall, *Ferroelectric and Antiferroelectric Liquid Crystals* (Wiley-VCH, Weinheim, 1999).
[12] R. Zbinden, *Infrared Spectroscopy of High Polymers* (Academic, New York, 1964).
[13] K. H. Kim, K. Ishikawa, H. Takezoe, and A. Fukuda, Phys. Rev. E **51**, 2166 (1995).
[14] K. Miyachi, J. Matsushima, Yo. Takanishi, K. Ishikawa, H. Takezoe, and A. Fukuda, Phys. Rev. E **52**, R2153 (1995).
[15] W. G. Jang, C. S. Park, J. E. Maclennan, K. H. Kim, and N. A. Clark, Ferroelectrics **180**, 213 (1996).
[16] A. Kocot, R. Wrzalik, B. Orgasinska, T. S. Perova, J. K. Vij, and H. T. Nguyen, Phys. Rev. E **59**, 551 (1999).
[17] A. A. Sigarev, J. K. Vij, Yu. P. Panarin, and J. W. Goodby, Phys. Rev. E **62**, 2269 (2000).
[18] A. Kocot, J. K. Vij, and T. S. Perova, in *Advances in Liquid Crystals*, edited by J. K. Vij, special issue of Adv. Chem. Phys. **113**, 203 (2000).
[19] N. M. Shtykov, J. K. Vij, R. A. Lewis, M. Hird, and J. W. Goodby, Phys. Rev. E **62**, 2279 (2000).
[20] V. M. Vaksman and Yu. P. Panarin, Mol. Mater. **1**, 147 (1992).
[21] L. M. Sverdlov, M. A. Kovner, and E. P. Krainov, *Vibrational Spectra of Polyatomic Molecules* (Israel Program for Scientific Translations, Jerusalem, 1974).
[22] A. Kocot, R. Wrzalik, and J. K. Vij, Liq. Cryst. **21**, 147 (1996).
[23] O. E. Panarina, Yu. P. Panarin, J. K. Vij, M. S. Spector, and R. Shashidhar, Phys. Rev. E **67**, 051709 (2003).
[24] J. Prost and R. Bruinsma, Ferroelectrics **148**, 25 (1993).